1

Store-operated calcium entry contributes to abnormal Ca^{2+} signalling in dystrophic mdx mouse myoblasts

Marta Onopiuk[2,4,*], Wojciech Brutkowski[1,2,*], Christopher Young[1], Elżbieta Krasowska[1,2] Justyna Róg[2], Morten Ritso[3], Sylwia Wojciechowska[2], Stephen Arkle[1], Krzysztof Zabłocki[2#$] and Dariusz C. Górecki[1#].

[1]School of Pharmacy and Biomedical Sciences, University of Portsmouth, Portsmouth, UK;

[2]Nencki Institute of Experimental Biology, Warsaw, Poland;

[3]Institute of Genetic Medicine, Newcastle University, Newcastle Upon Tyne, UK.

[4] Present address: Departments of Cell Biology, University of Oklahoma Health Sciences Center, Oklahoma City, Oklahoma, USA

* equal participation; # senior co-authors

$Corresponding author: K. Zabłocki, Nencki Institute of Experimental Biology, 3 Pasteura str. 02-093 Warsaw, Poland; e-,ail: k.zablocki@nencki.gov.pl

Keywords: Duchenne muscular dystrophy; mdx; myoblasts; store-operated calcium entry, STIM1 protein

Abbreviations: $[Ca^{2+}]_c$, cytosolic Ca^{2+} concentration; DMD, Duchenne muscular dystrophy; DMEM, Dulbecco's modified Eagles' medium; ER, endoplasmic reticulum; NCX, sodium/calcium exchanger; SOCE, store-operated Ca^{2+} entry; STIM1, stromal interaction molecule 1;TRPC, transient receptor potential channel canonical;

ABSTRACT

Sarcolemma damage and activation of various calcium channels are implicated in altered Ca^{2+} homeostasis in muscle fibres of both Duchenne muscular dystrophy (DMD) sufferers and in the mdx mouse model of DMD. Previously we have demonstrated that also in mdx myoblasts extracellular nucleotides trigger elevated cytoplasmic Ca^{2+} concentrations due to alterations of both ionotropic and metabotropic purinergic receptors. Here we extend these findings to show that the mdx mutation is associated with enhanced store-operated calcium entry (SOCE). Substantially increased rate of SOCE in mdx myoblasts in comparison to that in control cells correlated with significantly elevated STIM1 protein levels. These results reveal that mutation in the dystophin-encoding Dmd gene may significantly impact cellular calcium response to metabotropic stimulation involving depletion of the intracellular calcium stores followed by activation of the store-operated calcium entry, as early as in undifferentiated myoblasts. These data are in agreement with the increasing number of reports showing that the dystrophic pathology resulting from dystrophin mutations may be developmentally regulated. Moreover, our results showing that aberrant responses to extracellular stimuli may contribute to DMD pathogenesis suggest that treatments inhibiting such responses might alter progression of this lethal disease.

1. Introduction

Duchenne muscular dystrophy (DMD) is an incurable disorder caused by mutations in the DMD gene encoding dystrophin. Dystrophin localises to the cytoplasmic face of the muscle fibre sarcolemma and anchors a group of proteins known as the dystrophin-associated protein (DAP) complex to actin filaments and microtubules [1, 2]. These interactions provide a link between the cytoskeleton, DAP complex in the cell membrane and the extracellular matrix components bound by DAP and has a role in mechanical strengthening of the sarcolemma during the contractile activity [1]. While disruption of this link certainly contributes to DMD pathology, additional pathogenic mechanisms are also involved and include an abnormal calcium homeostasis; the cytosolic calcium ($[Ca^{2+}]_c$) concentration is raised in the subsarcolemmal region of dystrophic muscle cells and this cannot be explained by membrane ruptures alone [3]. This is particularly true in myoblast, which are non-excitable cells and do not have contractile apparatus, thus a rupture of their sarcolemma due to mechanical stress typical for differentiated muscle cells is not likely.

In our earlier studies we have shown that mutations of the dystophin gene exert a previously unrecognized effect on nucleotide-induced calcium responses in undifferentiated muscle cells. Exposure of the dystrophic (mdx) mouse myoblasts to extracellular ATP triggers a significant increase in $[Ca^{2+}]_c$, with both P2X and P2Y receptors involved. Probing the P2X (ionotropic) arm of

this abnormal purinergic response we identified P2RX7 as the main receptor responsible [4,5] and also discovered a novel mechanism of autophagic cell death evoked by activation of the P2RX7 large pore specifically in dystrophic myoblasts [6].

Stimulation of metabotropic P2Y receptors coupled with G_q protein initiates a signalling pathway, involving an activation of phospholipase C and increase of IP3 concentration, which activates Ca^{2+} release from the intracellular calcium stores in the sarcoplasmic reticulum. The latter is prerequisite for activation of store-operated calcium entry (SOCE); a depletion of the intracellular calcium stores activates Ca^{2+} entry from the extracellular milieu. The phenomenon of store-operated Ca^{2+} entry was discovered in the mid- 80's of the last century but the true mechanism of this process was not clarified until 20 years later [7, 8]. Among proteins involved in activation and regulation of SOCE, the two most prominent are STIM1 and Orai1. STIM1 spans the ER membrane and, thanks to the ER-hand domain located in the lumen of the ER cistern, senses Ca^{2+} concentration in stores. Depletion of the ER of calcium results in a horizontal movement of STIM1 in the ER membrane, its clustering and then interaction with the plasma membrane channel-forming protein Orai1. This, finally, results in Ca^{2+} entry into the cell. Replenishment of Ca^{2+} stores breaks these molecular interactions and stops Ca^{2+} influx [9, 10]. Furthermore, participation of different proteins of the TRP-family in activation of various routes of Ca^{2+} entry, including in SOCE, was also suggested [11, For review see: 12]. Given that our data indicated an abnormal calcium response of mdx myoblasts following stimulation of P2Y receptors [4] we decided to study whether this may, at least partially, result from up-regulation of SOCE. We have found a significantly increased activity of SOCE in mdx myoblasts, which was accompanied by increased levels of STIM1 protein. Interestingly, the expression of Orai1 protein was unchanged in these cells. Similarly, changes in the TRPC proteins levels could not explain accelerated Ca^{2+} entry upon depletion of the ER stores. While increased activity of SOCE in dystrophic myofibers was described earlier [13] the importance of data presented here stems from the fact that myoblasts, as undifferentiated muscle cells, do not produce the full-length dystophin protein at levels detectable by Western blot despite clearly expressing the full-length transcript. Thus, abnormalities in susceptibility to ATP described previously [4,5] as well as in the activity of store-operated calcium entry described here imply that focal dystrophin or its transcript alone may have a function. Its absence in Duchenne muscular dystrophy triggers an additional pathological mechanisms leading to an aberrant calcium homeostasis as early as in myoblasts. Understanding these processes may offer new therapeutic opportunities for the management of this lethal pathology.

2. Materials and methods

2.1. Cell culture

The mdx mouse and dystrophin-positive C57Bl10 myoblast cell lines were used. These two cell lines were derived from the "immorto mouse" or H2Kb-tsA58 line [14] and tested for their muscle phenotype and for myogenic potential following differentiation [5, 15, 16,]. Cells were cultured in Dulbecco's modified Eagles' medium (DMEM) supplemented with 20% foetal calf serum (FCS), 4 mM L-glutamine, 100 unit/ml penicillin, 100 g/ml streptomycin, and 20 unit/ml murine -interferon (Invitrogen, San Diego, CA,USA) at 33°C in a 95% air, 5% CO_2 atmosphere. When the cells reached 95% of confluence their myogenic properties could be confirmed by their ability to differentiation into myotubes. It was induced by changing the growth medium to the differentiation one containing 2% horse serum (HS) instead of FCS and depleted of -interferon and incubation at 37°C. Myotubes were examined after 3-6 days in culture. All media and reagents were purchased from Sigma (Poole, UK).

2.2. Primary myoblast culture

Mice were used with the approval of the local ethics commission (Polish Law on the Protection of Animals). Satellite cells were prepared from hindlimb muscle of control (C57BL/10ScSnJ) and dystrophic (C57BL/10ScSn-Dmd<mdx>/J) adult (2-3 month-old) male mice (Jackson Laboratory, Jacksonville, USA). Isolation and purification of satellite cells from tibialis anterior (TA) and soleus (Sol) muscles and myoblast culture procedures were performed as described in [17]. Briefly, whole muscles were sterilized in PBS with betadine and iodine and then digested with 0.2% collagenase type I in DMEM for 1.5 h at 37°C, rinsed in DMEM supplemented with 1 g/l glucose, 1 mM pyruvate, 4 mM L-glutamine, 10% HS, 0.5% chicken embryo extract (CEE), 1000 U/l penicillin (1000 U/l) and 1 mg/l streptomycin and triturated with pipettes of gradually decreasing diameter. Entire fibres were separated, rinsed four times with the same medium and finally transferred into DMEM (composition as above, supplemented with 20% FBS). Purified fibres were dispersed by forcing through an 18 guage injection needle, filtered through 40 m pore diameter nylon bolting cloth, put into collagen-coated culture dishes and incubated in the same medium at 37°C in humidified atmosphere of air (95%) and CO_2 (5%) for 5 days.

2.3. RT-PCR analysis

Total cellular RNA was extracted from myoblasts using RNA Isolation System (Promega, Southampton, UK) and 5 g of RNA were reverse transcribed using random hexamers and the Superscript First Strand Synthesis System (Fisher). Reverse transcriptase was omitted in negative control samples. RT-PCR was performed with primer sets specific for STIM1 transcripts: Fv: 5'-TGCTGTTTGGGCCTCCTCTC-3' and Rev: 5'-CCTCCACCTCATGGGTCAGC-3' based on [18].

PCR conditions for amplification were 94°C for 4 min, followed by 35 cycles of 94°C for 60 s, 58°-60°C for 60 s, 72°C for 60 s with a final extension step of 72°C for 7 min. The identity of the amplicons was confirmed by sequencing and restriction analysis. Semi-quantitative analyses of STIM1 expression were performed essentially as previously described [5]. All experiments were repeated at least 3 times and performed in triplicate.

2.4. Protein extraction and analysis

Proteins were extracted from adherent cells by scraping into extraction buffer (1x LysisM, 1x protease inhibitor cocktail, 2 x phosphatase inhibitor cocktail (all Roche), 2 mM sodium orthovanadate (Sigma) suspending with the use of automatic pipets and incubation of this suspension on ice for 20 min. After centrifugation (15 000 x g, for 20 min at 4°C) protein concentrations in supernatants collected were determined using a bicinchoninic acid assay kit (Sigma). Remaining supernatants were mixed with sample buffer at 3:1 $^v/_v$ ratio, heated for 5 min at 95 C and chilled on ice and stored at -80°C. Proteins were separated on SDS-polyacrylamide gels (6-12% $^w/_v$ depending on the molecular mass of protein) and electroblotted onto Hybond C membranes (Amersham, UK). Blots were blocked in 5% $^w/_v$ non-fat milk powder in 1x TBST, 0.01% $^v/_v$ Tween-20 (Sigma) for 1h prior to probing with appropriate primary antibody (for STIM1, NCX, SERCA1 and 2 from Alomone, or TRPC1, TRPC3 and TRPC6 from Abcam) or diluted in a blocking buffer containing 2% milk (for 1h at RT) then washed (3x) with 1x PBST for 10 min and incubated with the appropriate horseradish peroxidase-conjugated secondary antibody (Sigma) for 1h. Specific protein bands were visualized using luminol-based substrates (Uptlight US, Cheshire Sciences) and images obtained using a G- BOXChemi XT-16 system (Syngene). -actin antibody (Sigma) was used as a protein-loading control. Densitometric analyses of specific protein bands were made using exposure times within the linear range and the integrated density measurement function of Image J software. All experiments were repeated at least 3 times with similar results obtained in each replicate.

2.5. $[Ca^{2+}]_c$ measurements in myoblasts in vitro

Myoblasts were cultured on glass coverslips in a 6-well plate (500,000 cells/well) for 48 h under conditions described above. Cells (70-80% confluent) were loaded with 1 M Fura 2 AM (Molecular Probes, Oregon) in culture medium for 15 min at 33°C (in a case of immortalized cells) or with 2 M Fura 2AM diluted with the serum-depleted growth medium for 25 min at 37°C (primary myoblasts) in a humidified atmosphere of 95% O_2 and 5% CO_2. The cells were then washed twice with the solution composed of 5 mM KCl, 1 mM $MgCl_2$, 0.5 mM Na_2HPO_4, 25 mM HEPES, 130 mM NaCl, 1 mM pyruvate, 5 mM D-glucose, and 0.1 mM $CaCl_2$, pH 7.4 and the coverslips were mounted in a cuvette containing 3 ml of either the nominally Ca^{2+}-free assay solution (as above but 0.1 mM $CaCl_2$

was replaced by 0.05 mM EGTA) or Ca^{2+}-containing assay solution (as above but with 2 mM $CaCl_2$) and maintained at RT in a spectrofluorimeter (Shimadzu, RF5001PC).

Fluorescence was recorded at 510 nm with excitation at 340 and 380 nm. At the end of each experiment the Fura 2 fluorescence was calibrated by addition of 8 M ionomycin to determine maximal fluorescence followed by addition of EGTA to complete removal of Ca^{2+}. Cytosolic Ca^{2+} concentration $[Ca^{2+}]_c$ was calculated according to Grynkiewicz et al. [19]. The cells were treated with: 1 mM ATP (a P2 agonist); 1 µM Coomassie Brilliant Blue G 250 (CBB - a P2X7 antagonist applied 10 min prior to the addition of ATP); 1 M thapsigargin (SERCA inhibitor). Each experiment was repeated at least 5 times.

2.7. Analysis of results

Data are expressed as a mean value ± standard deviation (SD). Statistical significance was assessed by Student's t-test A p value of <0.05 was considered statistically significant where n=3-5 for PCR and Western data, and n=3-9 for other analyses. In the case of immortalised myoblasts "n" represents the number of independent experiments with cells derived from different passages. In the case of primary myoblasts it refers to the number of experiments with cells derived from different "n" animals (i.e. biological replicates).

2. Results

3.1 Myoblast calcium response to stimulation with nucleotides

We have analysed functional differences in store-operated calcium entry between wild-type (w/t) and dystrophic mouse myoblasts. These cells have been extensively characterized previously [5, 16,] and show myogenic characteristics upon differentiation (Fig 1). Stimulation of myoblasts placed in the calcium-free buffered salt solution with 1 mM ATP resulted in an immediate increase in cytosolic Ca^{2+} (Fig. 2A). This reflects calcium release from the intracellular stores, due to activation of a P2Y-evoked and protein G-mediated signalling pathway. More pronounced response in mdx myoblasts may suggest higher susceptibility of dystrophic cells to such an excitation than one shown by control myoblasts. Similar treatment of cells in the presence of extracellular Ca^{2+} also causes more intensive increase in cytosolic Ca^{2+} in mdx cells (Fig. 2B). In this case, increase in the cytosolic Ca^{2+} concentration may correspond not only to depletion of the ER stores but also to activated capacitive Ca^{2+} entry into cells, secondary to the calcium release. Moreover, ATP could, at least potentially, activate Ca^{2+} influx due to activation of ionotropic receptors belonging to the P2X family. However, as we have previously shown, the only functional receptor active in these cells being P2X7, it can be fully inhibited by CBB [4]. Thus, preincubation of cells with this inhibitor allowed selective

activation of metabotropic receptors and permitted distinguishing their responses from those of ionotropic ones (Fig. 2B). The important question, which of the P2Y receptor(s) is specifically responsible for the increased release of Ca^{2+} from intracellular stores in dystrophic myoblasts is currently unanswered. Nevertheless, stimulation of each of those cooperating with PLC in a G protein-mediated manner can activate similar chain of events involving depletion of intracellular calcium stores and subsequent activation of store-operated calcium entry (SOCE). Thus, receptor identity notwithstanding, the question arises whether enhanced Ca^{2+} influx into mdx myoblasts may, and to what extent, involve dystrophy-evoked stimulation of store-operated calcium entry as a second component of the cellular calcium response upon metabotropic stimulation of purinergic receptors. Therefore, subsequent experiments were focused on this question.

3.2. Alteration of store operated mechanisms in dystrophic myoblasts

To answer this question, cells placed in the calcium-free solution were treated with thapsigargin to irreversibly inhibit SERCA and completely deplete intracellular calcium stores. After depletion of the ER calcium stores and establishment of the cytosolic Ca^{2+} concentration at a stable level under calcium-free conditions, the assay medium was supplemented with 2 mM $CaCl_2$. Such approach allowed skipping first steps of cell activation (comprising of receptor stimulation, PLC activation, and IP_3 formation and Ca^{2+} release from the stores) and permitted investigating calcium entry independently of any primary extracellular stimulus and receptor activation. Thapsigargin-evoked total depletion of the ER calcium stores results in maximal activation of SOCE. Changes of fluorescence measured using the Fura-2 probe allow estimating the rate of Ca^{2+} entry seen as an initial slope of the curve representing increase in cytosolic Ca^{2+} concentration immediately after the addition of $CaCl_2$ into the assay. Using this approach we minimize any influence of other processes, which may affect an increase of cytosolic Ca^{2+} concentration as a direct result of accelerated Ca^{2+} entry As shown in Fig 3A and B we have found that Ca^{2+} entry into mdx cells was substantially faster than into respective w/t myoblast. It should be emphasized that an addition of $CaCl_2$ into the assay without preincubation of cells with thapsigargin was not followed by any Ca^{2+} influx to either w/t or mdx myoblasts (not shown). This excludes unspecific Ca^{2+} influx, which could affect thapsigargin-induced store-operated calcium. Moreover, the maximal Ca^{2+} concentration reached much higher levels in mdx then in control cells. However, this value may be strongly affected by processes lowering cytosolic Ca^{2+} concentrations because it delimits a point of equilibrium between calcium influx into and efflux from a cell. In addition, a feed-back inhibition of store-operated calcium channels by Ca^{2+} accumulated beneath the plasma membrane must be considered. Therefore, comparisons of the maximal values of calcium transients in control and dystrophic myoblasts do not seem to be a reliable measure of SOCE activity. This seems particularly remarkable in the view of

data shown in Fig. 3D indicating evidently enhanced levels of Na^+/Ca^{2+} exchanger (NCX), which is responsible for Ca^{2+} extrusion and recovery of the $[Ca^{2+}]_c$ resting level. This suggests that the value of $[Ca^{2+}]_c$ peak in mdx myoblasts might, in fact, be underestimated. In other words, the Ca^{2+} entry-counteracting process may be more efficient in the mdx then in the w/t cells. Actually, more precise analysis of traces derived from 15 independent experiments (one example shown in Fig. 3A) has revealed that the half-time of recovery of the cytosolic Ca^{2+} concentration to the new steady state is significantly shorter and that Ca^{2+} is removed much faster in mdx then in w/t myoblasts (Fig. 4). Moreover, mdx and w/t myoblasts differ in their response to thapsigargin. As shown in Fig. 3A, faster increase of the cytosolic Ca^{2+} concentration following addition of thapsigargin in mdx myoblasts may be correlated with significantly increased SERCA1 and SERCA2 protein levels (Fig. 3E and F), which may suggest more calcium being accumulated initially. Unchanged levels of IP3 receptor in mdx cells (Fig. 3C) do not allow attributing faster Ca^{2+} release to this protein. On the other hand, much faster decay of the Ca^{2+} transient to the basal level may reflect increased amount of NCX exchanger. Pre-treatment of cells with thapsigargin results in complete depletion of the ER stores and maximal activation of SOCE. Thus, differences in SERCA level did not seem to interfere with Ca^{2+} entry into cells, particularly as $CaCl_2$ was added into the assay buffer as soon as a new (very low and identical in both cell lines) basal concentration of Ca^{2+} was established. It should also be stressed that calcium release upon treatment of cells with thapsigargin is relatively slow. Therefore, the heights of $[Ca^{2+}]_c$ peak do not allow estimating the amount of calcium stored because changes in cytosolic Ca^{2+} concentrations are strongly influenced by the process of calcium removal. One likely explanation for the observed difference concerning rate of calcium entry upon supplementation of the assay with $CaCl_2$ could be that dystrophic cells exhibit more active SOCE due to higher levels of proteins crucially involved in this process. This possibility we studied using Western blotting analysis of major proteins participating in SOCE: STIM1 and Orai1. Furthermore, amounts of TRPC1, TRPC3 and TRPC6 (other proteins believed to participate in SOCE) were also tested in both w/t and mdx myoblasts. As shown in Fig. 5A, STIM1 protein levels in mdx myoblasts were substantially higher than it w/t cells. Similar phenomenon was observed at later stages of differentiation in healthy and dystrophic muscles [13]. On the other hand, semi-quantitative PCR assay has nor revealed any noticeable differences between the STIM1 transcript content in both cell lines used in this study (Fig. 5C). We also found that the total level of Orai1 protein was the same in both cell lines tested (Fig. 6). This observation is contrary to the data from differentiated muscle cells and indicate important differences in cellular calcium homeostasis during maturation of w/t and dystrophic muscles [13]. Also amount of TRPC1 and TRPC3 proteins, which are postulated to be involved in abnormal Ca^{2+} homeostasis in dystrophic adult muscle fibres [20,21,22] were unchanged or only insignificantly lowered in mdx myoblasts, while TRP6 protein content in dystrophic myoblasts was reduced

substantially (Fig. 6B). In summary, these data suggest that, Orai1 and TRPC1, 3 and 6 proteins seem not responsible for stimulated Ca^{2+} entry into mdx myoblasts, due to their unchanged or even reduced (TRPC6) expression in mdx myoblasts. However, an increased activity/altered distribution of these proteins despite their unaltered/reduced levels could not be definitely excluded.

To exclude cell-line specific effects, the experiments were repeated in a second set of immorto mdx and w/t cells (independently derived from different lines of H2Kb-tsA58 w/t and mdx mice) and the same responses were found.

Furthermore, to exclude the possibility that some of the effects were due to cell immortalization, primary myoblasts isolated from mdx and w/t tibialis anterior and soleus muscles were analysed to study the thapsigargin-induced Ca^{2+} entry (Fig. 6A and B). Also in this case, significant up-regulation of SOCE correlated with increased levels of STIM1 protein in dystrophic myoblasts isolated from these two different muscle groups (Fig 6C).Unfortunately, high fragility of the primary myoblasts even grown on specially coated surfaces, forced us to modify the assay in order to keep its time as short as possible following the addition of thapsigargin used for depletion of the ER calcium stores. Nevertheless, differences between rates of Ca^{2+} entry were evident irrespective of not always completely reaching a steady state prior to addition of $CaCl_2$. Importantly, preincubation of myoblasts with 2-APB, commonly used inhibitor of SOCE [23], abolished Ca^{2+} entry into both wt and mdx cells isolated from tibialis anterior, thus finally confirming participation of SOCE in the observed Ca^{2+} entry (data not shown). In summary, findings in primary muscle cells confirmed the aforementioned data in myoblast lines and ruled out the possibility that the up-regulation of SOCE in immortalized mdx myoblasts was an artefact of cell modifications.

3. Discussion

Paracrine or autocrine stimulation of muscle cells with ATP, which is released in small amounts in response to skeletal muscle physiological activity, modulates Ca^{2+} homeostasis and muscle plasticity via activation of P2 receptors [24]. However, although first indications of the functional significance of ATP receptors in skeletal muscle cells emerged in 1983 [25], our understanding of the roles of specific P2 receptors in this tissue started emerging only recently. It is beyond any doubts that Gq-linked nucleotide receptors are involved in muscle cell differentiation, regeneration and motility [26 27, 28, 29, 30 (and references cited herein)]. Interestingly, several P2 receptors were found differentially expressed in muscles at different stages of DMD pathology [30, 31]. Moreover, enhanced Ca^{2+} entry into dystrophic myofibers due to activation of various Ca^{2+} channels and transport mechanisms has been described repeatedly [13, 32]. Such abnormalities are believed to be a result of impaired scaffolding of membrane proteins involved in Ca^{2+} signaling due to the absence of dystrophin-associated protein complexes [33]. These observations have been expanded by us and

others showing that mutations in dystrophin gene closely correlate with alteration of ATP signaling and that this abnormality affects myoblasts [4, 5] and lymphoblasts [34]. While convincing identification of Gq-linked P2Y receptor(s) producing the ATP-evoked abnormal Ca^{2+} increases in dystrophic myoblasts requires further studies, an enhanced metabotropic response to nucleotide stimulation is beyond any doubt.

We have found that the metabotropic purinergic response was significantly higher in dystrophic versus control cells both in the absence and in the presence of extracellular Ca^{2+} but in the latter case the relative stimulatory effect was more pronounced (see Fig. 2). This observation indicated that mdx myoblasts are more susceptible not only to nucleotide-induced Ca^{2+} release, but also that Ca^{2+} influx from the extracellular milieu, secondary to the Ca^{2+} release from the ER, is more effective in these cells.

Increased SOCE activity may contribute to cellular responses to numerous stimuli. Amongst these stimuli are nucleotides interacting with specific P2Y receptors. More abundant STIM1 protein found in dystrophic myoblasts compared to w/t cells partially explains the more intense calcium response in these cells when excited with nucleotides. On the other hand, enhanced Ca^{2+} release from the ER stores in mdx myoblasts stimulated with ATP in the absence of extracellular calcium clearly shows that SOCE per se is not the only over-activated component of metabotropic response in these cells. Undoubtedly however, SOCE participates in generation of abnormal calcium signals in dystrophic myoblasts exposed to multiple stimuli acting via depletion of the intracellular calcium stores. Enhanced SOCE into muscle fibres with the mutated dystrophin gene has been described previously. It was attributed to various mechanisms, including an impaired dystrophin/ 1-syntrophin scaffold formation [35] and increased STIM1 and Orai1 protein levels [13]. However, it must be stressed that these DMD studies were performed in differentiated muscle cells (myotubes and myofibers) and not in myoblasts used in our study, which are very different structurally and functionally.

Previously, we have shown that mitochondrial membrane potential in dystrophic cells is higher than in controls [36]. This could imply more efficient mitochondrial buffering of calcium ions which reduces a feedback inhibition of SOCE by Ca^{2+} accumulated in the close vicinity of the calcium channels [37]. However, dissipating mitochondrial potential with protonophore (CCCP), although resulting in a substantial inhibition of SOCE, did not abolish the difference between w/t and dystrophic myoblasts (data not shown). It suggests that the cause of the observed difference lies elsewhere.

In this study, the overstimulation of SOCE in dystrophic cells has been correlated with the increased STIM1 protein content. This difference was observed both between immortalized and primary dystophic and control myoblasts, thus excluding potential side-effect of immortalization. Therefore,

the more effective SOCE in dystrophic myoblasts could, at least to some extent, depend on differences in the levels of this crucial store-operated Ca^{2+} channel protein.

Interestingly, SOCE is of great importance in differentiating myoblasts and increasing levels of STIM1 correlate with accelerated muscle differentiation [38]. Consequently, it was shown that overexpression of STIM1 stimulates muscle cell differentiation, while silencing it inhibits this process [39]. Thus, it appears possible that the more active SOCE/higher STIM1 levels in dystrophic myoblasts reflect their higher "readiness" for differentiation described by others [40, 41] and also seen by us. Such over-activation of SOCE upon dystrophic cell stimulation might lead to cellular calcium overload and to increased susceptibility to cell death thus contributing to progressive muscle degeneration [43 (and references cited herein)].

It remains to be tested whether the elevated NCX content in dystrophic cells shown here is accompanied by its higher activity and reflects a defence mechanism protecting these cells against excessive calcium accumulation. If so, this mechanism could participate in cell adaptations enhancing their viability, as has been suggested elsewhere [42 (and references cited herein)]. In addition, substantially increased thapsigargin-induced SOCE rate in dystrophic mdx myoblasts could be underestimated because of the increased NCX levels in these cells.

Significantly elevated STIM1 protein level has also been found in situ, in fully differentiated dystrophic muscle fibres from the extensor digitorum longus muscle [13]. We have extended this observation by finding increased STIM1 levels in myoblasts of two other mouse leg muscles: soleus and tibialis anterior. These data show the same pattern of dystrophy-induced changes in both undifferentiated myoblasts and fully matured muscle cells. Conversely, dystrophin deficiency was also found to be accompanied by increased amount of Orai1, the second crucial protein involved in SOCE [13] while data shown here does not confirm this effect. It may suggest that a profile of changes concerning molecules involved in shaping the intracellular calcium homeostasis during muscle differentiations is strongly dependent on mutations in the dystrophin gene.

However, it must be stressed that while in differentiated muscle cells (myotubes and myofibers) the dystrophin protein presence was confirmed, in myoblasts used in our study, dystrophin protein is undetectable using standard Western blotting methods. Thus, an interpretation of the observed differences implying the impaired dystrophin-dependent scaffold formation seems to be unsatisfactory. Several experiments addressing this problem could be envisaged.

Considering the causative link between the disruption of the DAP complex or between DAP and its interacting proteins in dystrophic myotubes and the alteration of calcium homeostasis there, it has been shown that over-expression of mini- or full-length dystrophin improved calcium handling in cultured myotubes [43, 44]. It would be interesting to test whether expression of such mini-genes in myoblasts reduces intensity of SOCE to the control level.

Data presented here contest the conventional belief that mutations in dystrophin-encoding gene do not affect undifferentiated muscle cells. In all the experiments in this study, wild type and dystrophic myoblasts were tested outside their respective muscle environments, following a period of culture in vitro and so all the observed differences must have an intrinsic origin. The only difference between these cells is the presence or absence of the fully-functional Dmd gene. Therefore, results presented here add to a set of data challenging the current belief that mutations in this dystrophin-encoding gene do not affect undifferentiated muscle cells but only differentiated myotubes and myofibres. In contrast with this dogma, several studies conducted by us and others showed that dystrophic myoblasts similarly as in the case of lymphoblasts differ from wild type cells [4, 5, 34, 45]. For example, mdx myoblasts have altered expression and function of P2X7 receptors, leading to abnormal Ca^{2+} influx, ERK phosphorylation [4,5] and triggering a unique mechanism of autophagic cell death [6]. Moreover, dystrophin knockdown in adult muscles did not produce any pathology indicating that early dystrophin expression is crucial [46]. Indeed, examination of myogenesis revealed that this pathology starts in embryonic development arising from the loss stem cell. Thus, dystrophin expression appears to be essential for emergent stem cell function(s) and it has been shown that its absence alters myoblast differentiation processes [47] and their energy homeostasis [36]

DMD studies have been conducted using myotubes or myofibers, which reflected observations that while myoblasts contain dystrophin transcripts, these cells have little or any detectable protein [48, 49, 50]. Therefore, no phenotypic consequences of the protein absence due to mutations in the dystrophin gene were to be expected. Contrary to this, Ferrari et al., (1994) showed that DMD lymphoblasts (also expressing mRNA but with undetectable dystrophin protein levels) are more susceptible to ATP damage [34], exactly as the dystrophic myoblasts are. It is currently not known whether these effects are mediated by the residual protein or dystrophin mRNA-dependent regulatory pathways: An interesting alternative to the structural/scaffolding role of a trace amounts of dystrophin protein could be that the dystrophin transcript, which is absent in mdx cells due to nonsense-mediated decay, plays an important regulatory role in myoblasts.

To conclude, data described hitherto indicate that mutation in the dystrophin-encoding gene results in multiple phenotypic alterations that extend beyond structural stability of muscle fibre sarcolemma and clearly can also demonstrate as early as in undifferentiated myoblasts. The increased SOCE due to enhanced STIM1 level together with purinergic abnormalities occurring in dystrophic myoblasts could affect muscle regeneration and thus exacerbate the disease phenotype.

References

[1] I. Dalkilic, L.M. Kunkel, Curr. Opin. Genet. Dev. 13 (2003) 231-238.

[2] K.W. Prins, J.L. Humston, A. Mehta, V. Tate, E. Ralston, J.M. Ervasti, J. Cell Biol. 186 (2009) 363-369.

[3] B. Constantin, S. Sebille, C. Cognard, J. Muscle Res. Cell Motil. 27 (2006) 375-3863.

[4] D. Yeung, K. Zablocki, C-F. Lien, T. Jiang, S. Arkle, W. Brutkowski, J. Brown, H. Lochmuller, J. Simon, E.A. Barnard, D.C. Gorecki,   FASEB J. 20 (2006) 610-620.

[5] C. Young, W. Brutkowski, C-F. Lien, S. Arkle, H. Lochmuller, K. Zablocki, D.C. Gorecki, J. Cell. Mol. Med. 16 (2012)1026-1037.

[6] C. Young, A. Sinadinos, A. Lefebvre, P. Chan, S. Arkle, D. Vaudry D.C. Górecki, Autophagy. (2014) in press.

[7] J.W. Putney Jr, Cell Calcium 7 (1986) 1-12.

[8] J. Soboloff, M.A. Spassova, X.D. Tang, T. Hewavitharana, W. Xu, D.L. Gill, J. Biol. Chem. 281 (2006) 20661-20665.

[9] A. Gudlur, Y. Zhou, P.G. Hogan, Curr. Top. Membr. 71 (2013) 33-58.

[10] J.T. Smyth, S.Y. Hwang, T. Tomita, W.I. DeHaven, J.C. Mercer, J.W. Putney, J. Cell. Mol. Med. 14 (2010) 2337-2349.

[11] Y. Liao, C. Erxleben, E. Yildirim, J. Abramowitz, D.L. Armstrong, L. Birnbaumer, Proc. Natl. Acad. Sci. USA 104 (2007) 4682-4687.

[12] K. Venkatachalam, C. Montell, Annu. Rev. Biochem. 76 (2007)387-417.

[13] J.N. Edwards, O. Friedrich, T.R. Cully, F. von Wegner, R.M. Murphy, B.S. Launikonis, Am. J. Physiol. Cell Physiol., 299 (2010) 42-50.

[14]J.E. Morgan, J.R. Beauchamp, C.N. Pagel, M. Peckham, P. Ataliotis, P.S. Jat, M.D. Noble, K. Farmer, T.A. Patridge, Dev. Biol. 162 (1994) 486-498.

[15] C. Brun, D. Suter, C. Pauli, P. Dunant, H. Lochmüller, J.M. Burgunder, D. Schumperli, J. Weis, Cellular Molec. Life Sci. 60 (2003) 557-566.

[16] L.H. Jørgensen, N. Larochelle, K. Orlopp, P. Dunant, R.W. Dudley, R. Stucka, C. Thirion, M.C. Walter, S.H. Laval, H. Lochmuller, Hum. Gene. Ther. 20 (2009) 641-650.

[17] A. Musarò, L.Barberi. Methods Mol.Biol. 633 (2010) 101-111.

[18] L. Wang, S. Takaku, P. Wang, D. Hu, S. Hyuga, T. Sato, S. Yamagata, T. Yamagata, Glycoconj. J. 23 (2006) 303-315.

[19] G. Grynkiewicz, M. Poenie, R.Y. Tsien, J. Biol. Chem. 260 (1985) 3440-3450.

[20] D.P. Millay, S.A. Goonasekera, M.A. Sargent, M. Maillet. B.J. Aronow, J.D.Molkentin, Proc. Nat. Acad. Sci USA 106 (2009) 19023-19028.

[21] C. Vandebrouck, D.Martin, M. Colson-Van Schoor, H. Debaix, P. Gailly, J. Cell. Biol. 158 (2002) 1089-1096.

[22] A. Patel, R. Sharif-Naeini, J. R. H. Folgering, D. Bichet, F. Duprat, E. Honoré, Pflugers Arch - Eu.r J. Physiol. 460 (2010) 571-581.

[23] M. Prakriya, R.S. Lewis, J. Physiol. 536 (2001), 3-19.

[24] S. Buvinic, G. Almarza, M. Bustamante, M. Casas, J. López, M. Riquelme, J.C. Saez, J.P. Huidobro-Toro, E. Jaimovich, J. Biol. Chem. 284 (2009) 34490-34505.

[25] H.A. Kolb, M.J.Wakelam, Nature 303 (1983) 621-623.

[26] G.P. Szigeti, H. Szappanos, T. Deli, J. Cseri, L. Kovacs, L. Csernoch, Pflugers Arch. 453 (2007) 509-518.

[27] M. Ryten, A. Hoebertz, G. Burnstock, Dev. Dyn. 221 (2001) 331-341.

[28] M. Ryten, P.M. Dunn, J.T. Neary, G. Burnstock, J. Cell Biol. 158 (2002) 345-355.

[29] T. Martinello, M.C. Baldoin, L. Morbiato, M. Paganin, E. Tarricone, G. Schiavo, E. Bianchini, D. Sandona, R. Betto, Mol. Cell. Biochem. 351 (2011) 183-196.

[30] C. Young, A. Sinadinos, D.C. Górecki,. WIREs Membr. Transp. Signal.   (2013) doi: 10.1002/wmts.96.

[31] T. Jiang, D. Yeung, C-F. Lien, D.C. Górecki, Neuromuscular Dis. 15 (2005) 225-236.

[32] R. Harisseh, A. Chatelier, C. Magaud, N. Déliot, B. Constantin, Am. J. Physiol. Cell Physiol. 304 (2013) C881-894.

[33] J. Sabourin, R. Harisseh, T. Harnois, C. Magaud, N. Bourmeyster, N. Déliot, B. Constantin, Cell Calcium 52 (2012) 445-56.

[34] D. Ferrari, M. Munerati, L. Melchiorri, S. Hanau, F. Di Virgilio, O.R. Baricordi, J. Am. Physiol. 267 (1994) C886-892.

[35] A. Vandebrouck, J. Sabourin, J. Rivet, H. Balghi, S. Sebille, A. Kitzis, G. Raymond, C. Cognard, N. Bourmeyster, B. Constantin, FASEB J. 21 (2007) 608-617.

[36] M. Onopiuk, W. Brutkowski, K. Wierzbicka, S. Wojciechowska, J. Szczepanowska, J. Fronk, H. Lochmuller, D.C. Górecki, K. Zablocki, Biochem. Biophys. Res. Commun. 386 (2009) 463-466.

[37] K. Zabłocki, A. Makowska, J. Duszyński, Cell Calcium 33 (2003) 91-99.

[38] T. Li , E.A. Finch , V. Graham , Z.S. Zhang , J.D. Ding , J. Burch , M. Oh-hora , P. Rosenberg, Mol. Cell. Biol. 32 (2012) 3009-3017.

[39] B. Darbellay, S. Arnaudeau, S. Konig, H. Jousset, C. bader, N. Demaurex, L. Bernheim, J. Biol. Chem. 284 (2009) 5370-5380.

[40] Z. Yablonka-Reuveni, Anderson, J.E. Dev. Dyn. 235 (2006) 203-212.

[41] S. Kiviluoto, J.P. Decuypere, H. De Smedt, L. Missiaen, J.B. Parys, G. Bultynck, Skelet. Muscle 1(2011) doi: 10.1186/2044-5040-1-16.

[42] D. Khananshvili, Mol. Aspects Med. 34 (2013) 220-235.

[43] H. Balghi, S. Sebille, L. Mondin, A. Cantereau, B. Constantin, G. Raymond, C. Cognard, J. Gen. Physiol. 128 (2006) 219-230.

[44] A. Vandebrouck, T. Ducret, O. Basset, S. Sebille, G. Raymond, U. Ruegg, P. Gailly, C. Cognard, B. Constantin, FASEB J. 20 (2006)136-138.

[45] R. Rawat, T.V. Cohen, B. Ampong, D. Francia, A. Henriques-Pons, E.P. Hoffman, K. Nagaraju, Am. J. Pathol. 176 (2010) 2891-2900.

[46] M.M. Ghahramani Seno, I.R. Graham, T. Athanasopoulos, C. Trollet, M. Pohlschmidt, M.R. Crompton, G. Dickson, Hum. Mol. Genet. 17 (2008) 2622-2632.

[47] D. Merrick, L.K. Stadler, D. Larner, J. Smith, Dis. Model Mech. 2 (2009) 374-388.

[48] F. Trimarchi,   S. Fulle, L. Magaudda, C. Puglielli, S. Di Mauro, Cells Tissues Organs. 183 (2006) 87-98.

[49] A.F. Miranda, E. Bonilla, G. Martucci, C.T. Moraes, A.P. Hays, S. Di Mauro, Am. J. Pathol. 132 (1988) 410-416.

[50] Y.C. Park-Matsumoto, N. Kameda, T. Kobayashi, H. Tsukagoshi, Brain Res. 565 (1991) 280-289.

FIGURE LEGENDS

Fig. 1 Characterisation of immortalised muscle cell lines

Desmin immunodetection (green, top row panels) at specific time points (days) during the in vitro differentiation process illustrates the myogenic potential of immorto cell lines. Bottom panels show corresponding bright field images.

Fig. 2. Ca^{2+} response to ATP stimulation in immortalized wild type (w/t) and dystrophic (mdx) myoblasts

Representative traces from one typical experiment out of six: A. in the absence of extracellular Ca^{2+}; B. in the presence of 2 mM $CaCl_2$ in the assay Concentrations used: ATP - 1 mM; CBB - 1 M.

Fig. 3. Store-operated Ca^{2+} entry and changes in NCX and SERCA content in immortalized (w/t) and dystrophic (mdx) myoblasts

Cells incubated in the Ca^{2+}-free buffered saline solution were treated with 100 nM thapsigargin. After $[Ca^{2+}]_c$ recovery 2 mM $CaCl_2$ was added to the assay. A. Representative traces from one experiment out of 15; B. Mean rate of $[Ca^{2+}]_c$ increase after addition of $CaCl_2$ calculated as a slope of the initial part of the curve. Data show mean value ± SD from 15 independent experiments. * p < 0.01. C. Representative Western blotting of IP3; one out of 3 independent experiments. D. Western blotting analysis of NCX protein. Bottom bands represent protein loading controls (-actin). A representative result from one out of 3 experiments is shown. E and F. Western blotting analysis of SERCA1 and SERCA2 proteins, respectively. Shown are representative results from one of 3 independent experiments and respective mean values normalised to -actin ± SD. p < 0.003.

Fig. 4. Half-time necessary to attain a new steady state after the store-operated dependent calcium transient and rate of Ca^{2+} extrusion from cells in w/t and mdx immortalized myoblasts

A. A conceptual schematics showing how the half time of recovering the new was calculated

B. A half time for a new $[Ca^{2+}]_c$ steady state to be achieved

C. Initial rate of calcium efflux calculated as a slope of the initial part of curve after the maximal $[Ca^{2+}]_c$ was reached.

B and C: Mean values ± SD for 15 independent experiments. * p < 0.003, ** p < 0.05.

Fig. 5. STIM1 analyses in (w/t) and dystrophic (mdx) immortalized myoblasts

A. One representative Western blot out of 15 showing the relative amounts of STIM1 protein.

B. Mean STIM1 protein levels in control (assumed as 100%) and mdx myoblasts, expressed in a relation to actin, based on the data from 15 independent experiments; Data show mean value ± SD for the Western blots data obtained with the use of antibodies specific to the N-terminus of STIM1 protein. *p < 0.004 C. Agarose gel image representative of results obtained in semi-quantitative RT-PCR for STIM1 mRNA.

Fig. 6 Orai1 and TRPC proteins level in (w/t) and dystrophic (mdx) immortalized myoblasts

A. Representative single Western blot out of 10 showing the relative amount of Orai1 protein and mean value ± SD. Western blot data obtained with the use of antibodies specific to the N-terminus of Orai1 protein.

B. Representative single Western blot out of 3 showing the relative amounts of TRPC1, TRPC3 and TRPC6 proteins and mean values ± SD for these independent experiments. * p < 0.03
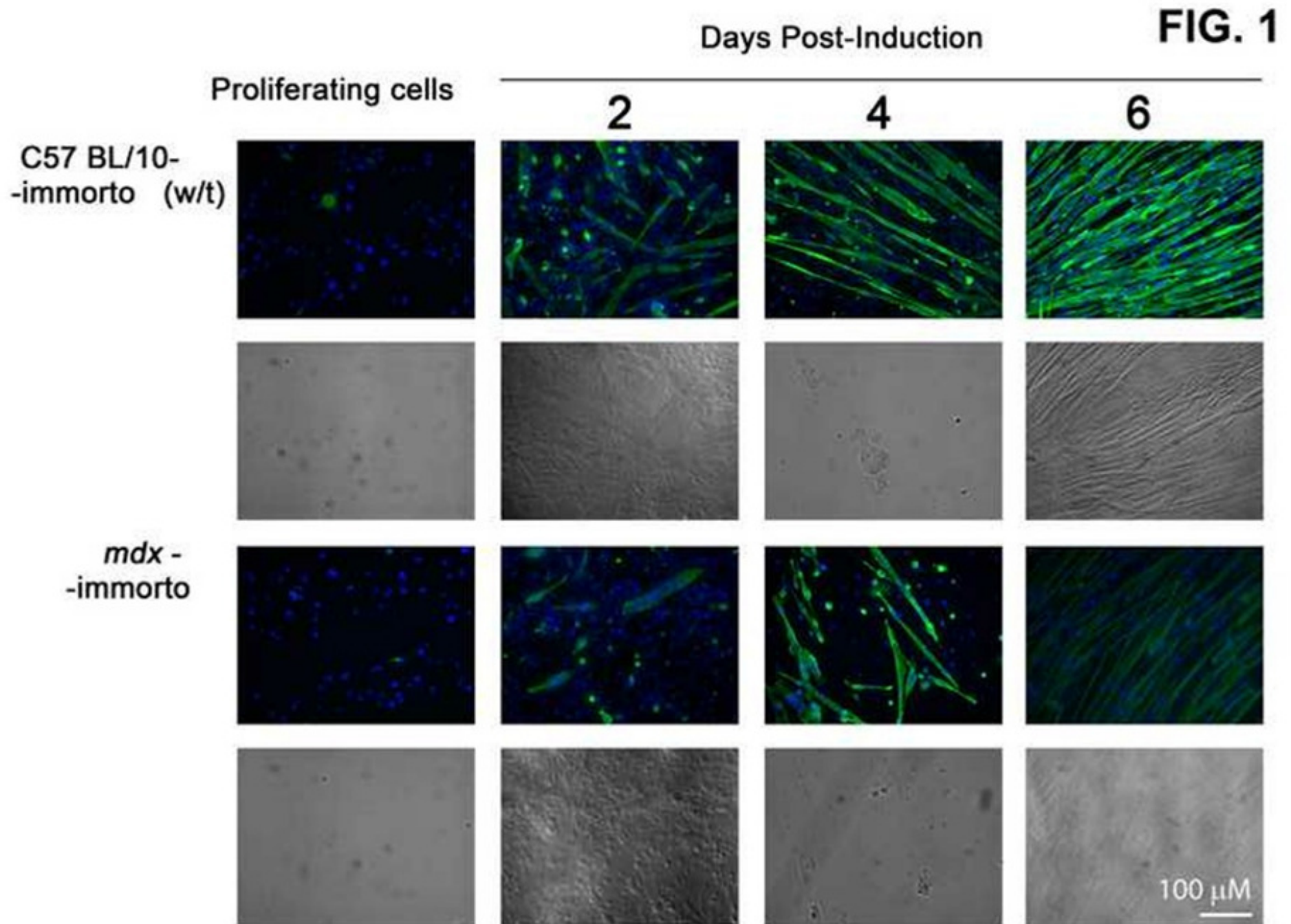
Fig. 7. Store-operated Ca^{2+} entry into primary w/t and mdx myoblasts derived from various muscles

Cells incubated in the Ca^{2+}-free buffered saline solution were treated with   100 nM thapsigargin. After $[Ca^{2+}]_c$ recovery, 2 mM $CaCl_2$ was added to the assay. A. representative traces from one experiment out of 5. B. Mean rate of $[Ca^{2+}]_c$ increase after addition of $CaCl_2$, calculated as a slope of the initial part of the curve; Data show mean value ± SD from 5 independent experiments. * p < 0.03. C. Western blot analyses of STIM1 levels in myoblast derived from various muscles: Sol, Soleus; TA, Tibialis anterior. Representative data from two experiments out of 5 are shown.

FIG. 1

Days Post-Induction

Proliferating cells

2   4   6

C57 BL/10- -immorto (w/t)

mdx - -immorto

100 µM

Fig. 2

Fig. 3

Fig. 4

Figure 5
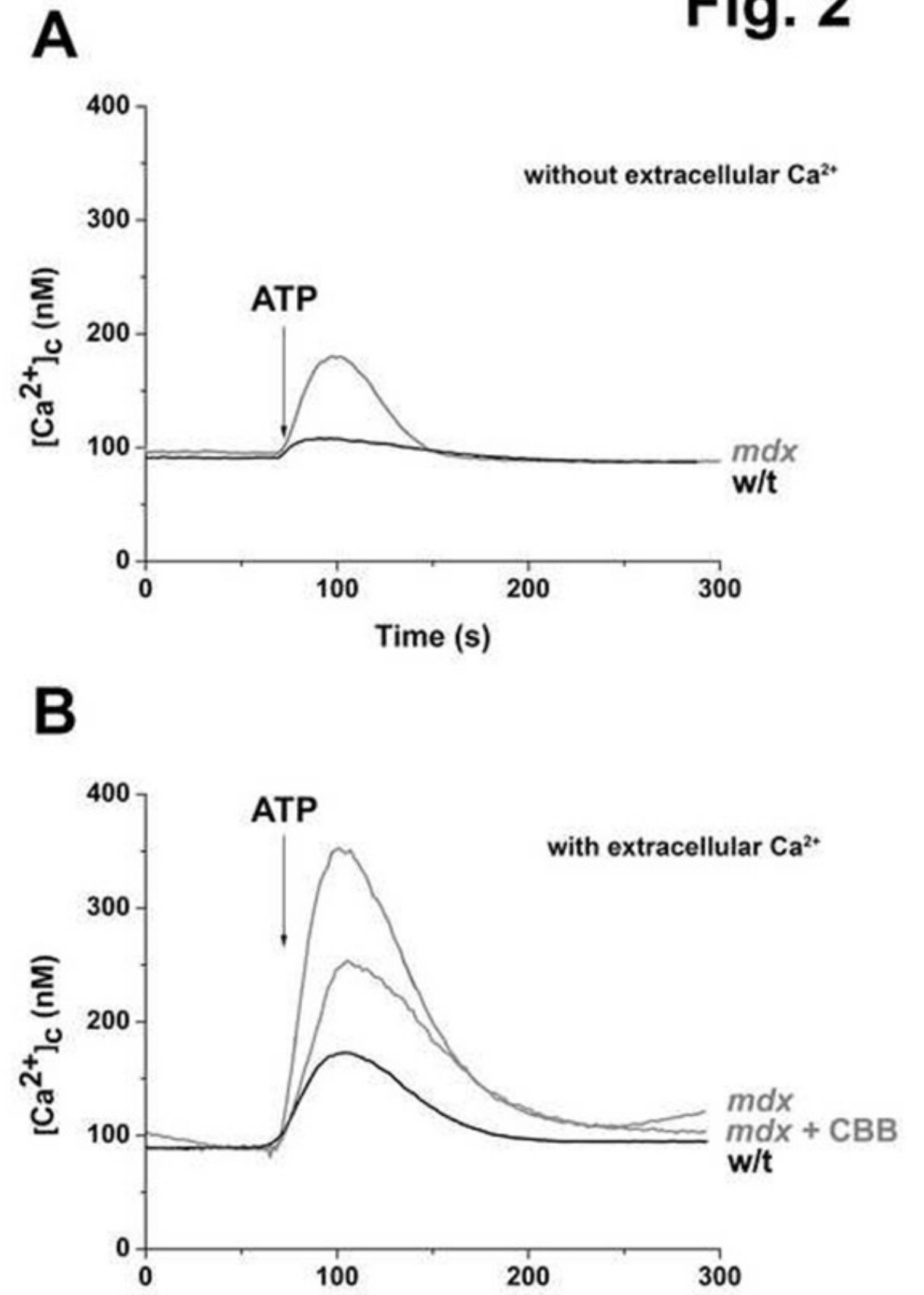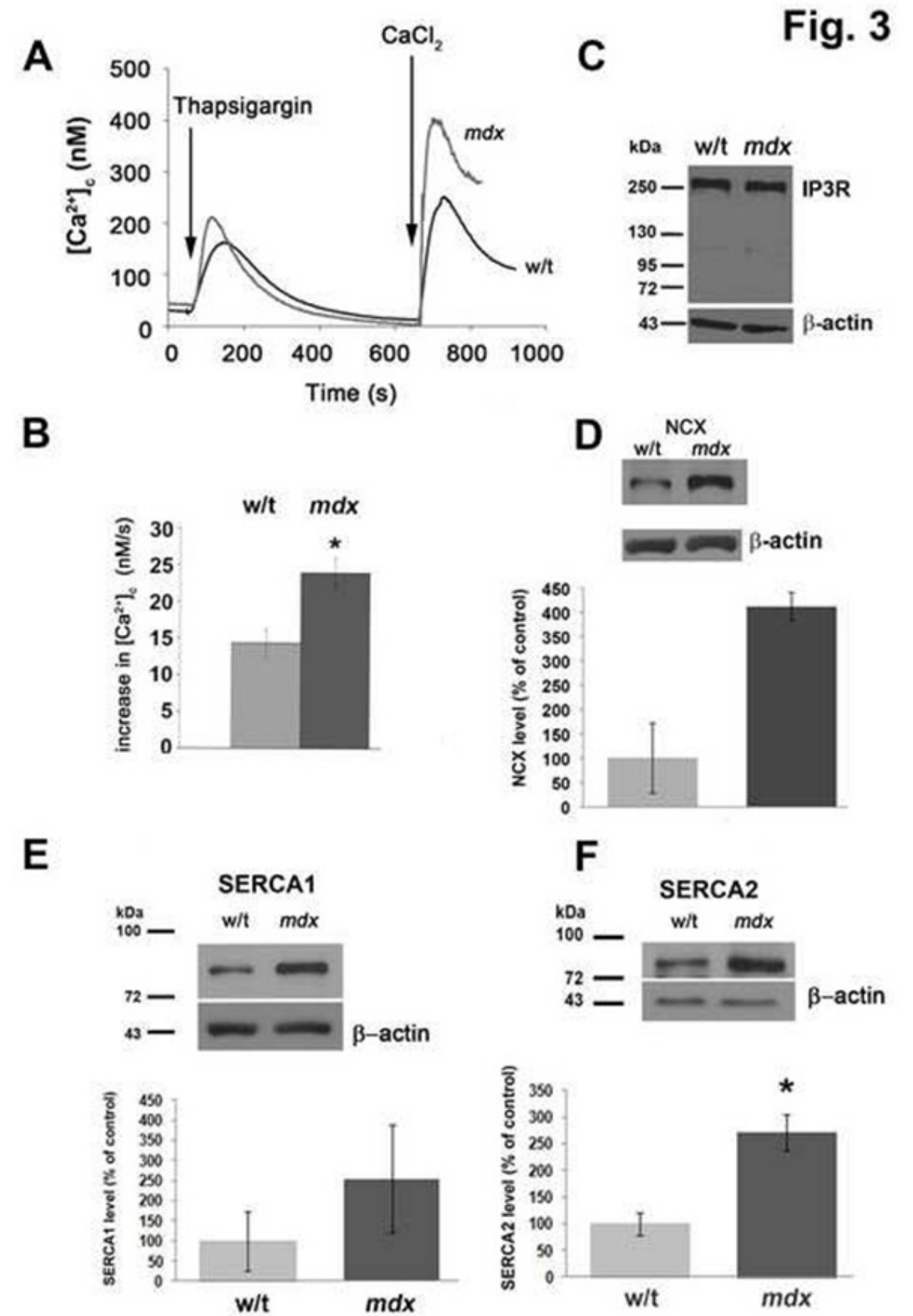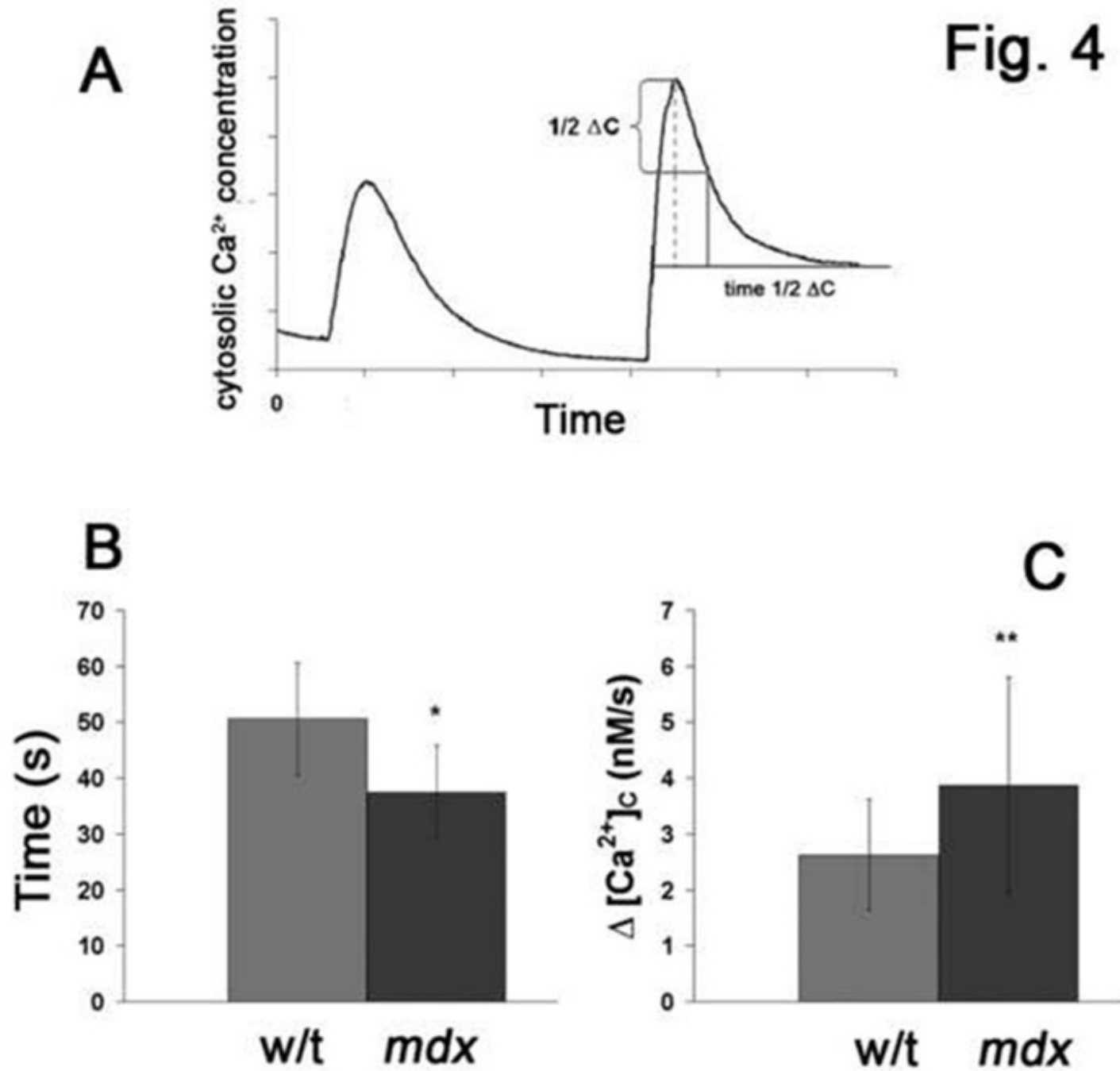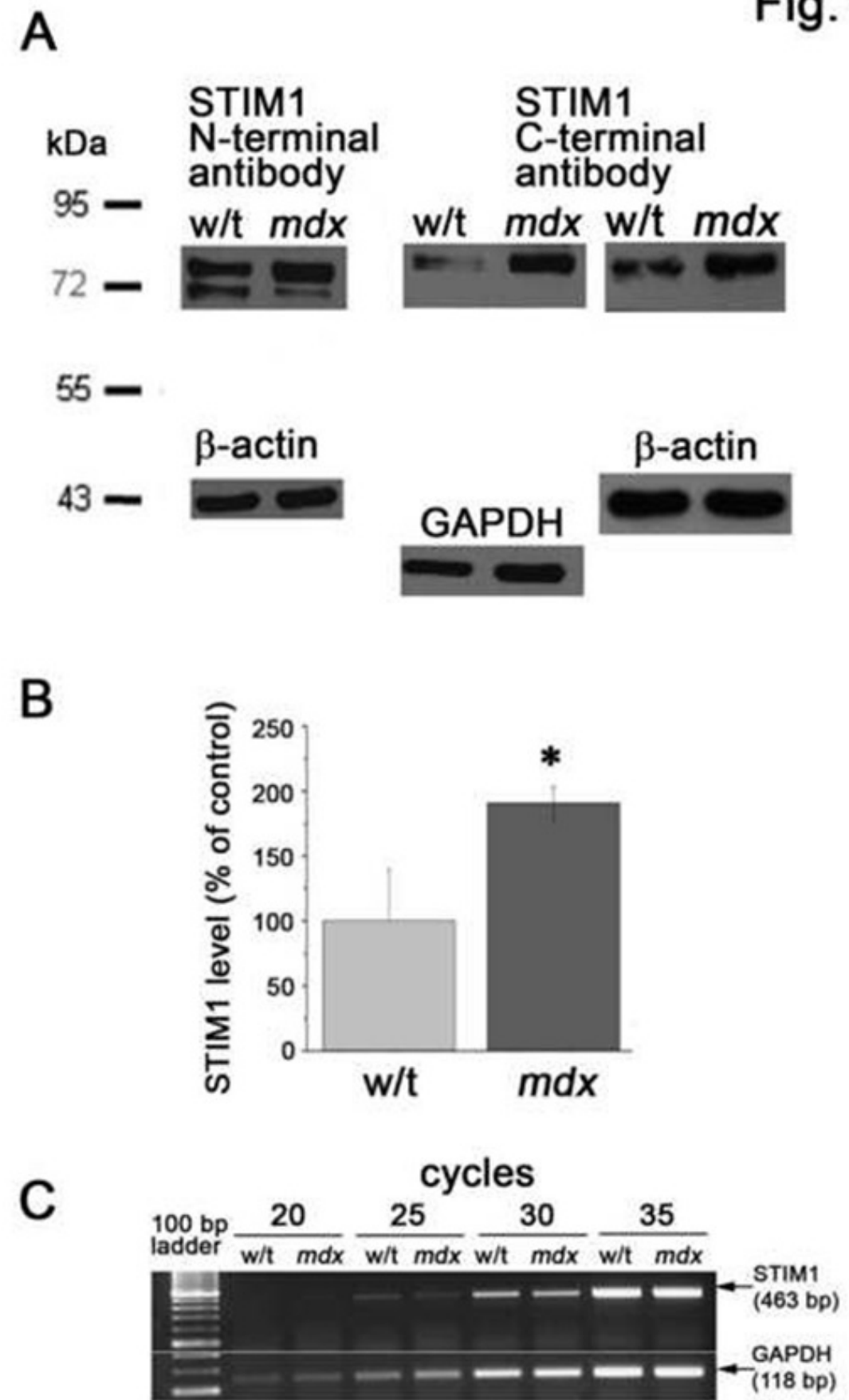**Click here to download high resolution image**

Fig. 5

Figure 6
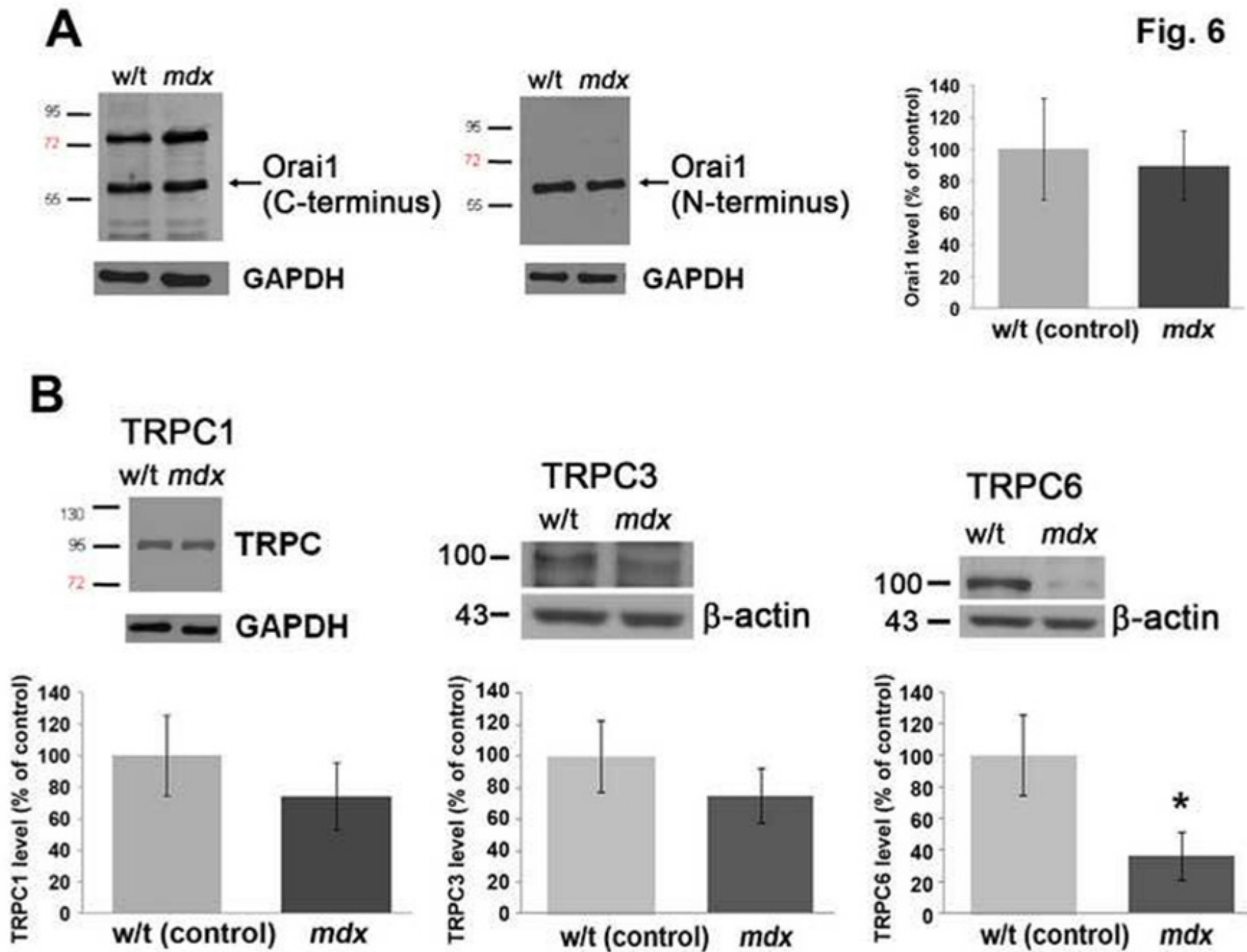**Click here to download high resolution image**

Figure 7
Click here to download high resolution image

Fig. 7